IET Communications

Research Article

IET Journals
The Institution of Engineering and Technology

Stability of S-Aloha with variable propagation delay

ISSN 1751-8628
Received on 17th April 2018
Revised 2nd April 2019
Accepted on 15th April 2019
doi: 10.1049/iet-com.2018.5224
www.ietdl.org

Priyatosh Mandal[1], *Swades De*[2] ✉

[1]*Centre for Development of Telematics, New Delhi, India*
[2]*Department of Electrical Engineering and Bharti School of Telecom, Indian Institute of Technology Delhi, New Delhi, India*
✉ *E-mail: swadesd@ee.iitd.ac.in*

Abstract: State-of-the-art variants of slotted Aloha (S-Aloha) for underwater acoustic networks do not consider the joint effect of retransmission and distance-dependent propagation delay variability, which is one of the most important parameters that affect the performance of any medium access control protocol. In this study, the authors analyse the stability of S-Aloha in a network environment, such as underwater, where propagation delay and its variance are not negligible. A finite number of unbuffered transmitters are considered. Through mathematical analysis, supported by discrete event simulations, they compare the utilisation and stability with S-Aloha in radio frequency environments where propagation delay, as well as delay variance, are negligible. The comparison results indicate that the stability region is appreciably shifted and also there is a significant decrease of utilisation in the presence of retransmission and distance-dependent propagation delay variability.

Nomenclature

R	max nodal communication (transmit/receive) range (m)
$r_{\min}$	min nodal communication (transmit/receive) range (m)
v	underwater acoustic signal propagation speed (m/s)
N	total number of users in the system
k	number of backlogged users in the system
p	transmission probability
α	retransmission probability
b_w	bandwidth of communication
T_s	slot time, s
T_t	packet transmission time, $s = \frac{\text{packet size}}{b_w}$
$T_p^{(r)}$	mean propagation delay when transmitter–receiver distance is r
$\sigma^{(r)}$	propagation delay deviation when transmitter–receiver distance is r
β	slot increment factor
q	propagation delay variability exponent
$P_s(k)$	packet reception success probability with k backlogged users in the system
D_k	drift when the number of backlogged users in the system is k

1 Introduction

Underwater acoustic sensor networks are targeted for monitoring of aquatic activities or changes. There are several unique differences between underwater networks and radio frequency (RF) networks. The main distinctive features from the perspective of medium access control (MAC) layer design are

(a) High and variable propagation delay: In underwater acoustic networks, signal propagation speed is 1500 m/s, which can vary with temperature, depth, and salinity of the water. The propagation speed is in the range [1460, 1520] [1]. This is one of the differences with the RF networks where signal propagation speed is about 3×10^8 m/s and there is no significant variation of propagation speed.
(b) Limited bandwidth: In an underwater network, with the increase of carrier frequency transmission loss increases. Owing to this fact, carrier frequency in the underwater network is in the sonar range, which is significantly lower than that in RF-based terrestrial wireless communication networks. As a consequence, the channel bandwidth of underwater networks is a few orders of magnitude lower than that of the terrestrial wireless networks [2].

Owing to variable propagation delay in underwater acoustic networks, the transmitter cannot predict the time of data reception perfectly at the gateway. This results in imperfect synchronisation and degradation of channel access performance. Also, due to remote/inaccessible deployments, recharging or battery replacement of the underwater field sensor nodes is difficult. Consequently, the employed MAC protocol needs to be energy-efficient so as to increase the lifetime of the sensor nodes.

MAC protocols can be categorised as random access based, reservation based, and collision-free protocols (time-division/frequency-division/code-division multiple access). Generally, random access protocols are preferred when the nodes are lightly loaded or when the data packets are of small size. When using random access protocols for large-sized data packet transmissions, collision-related losses are wasteful from energy as well as bandwidth resources perspectives. The collision-related losses are more prominent in the environments with propagation delay uncertainty. Therefore, for large data packet transmission, some kind of reservation protocol is used, while the reservation of channel is done via random access protocols carrying small reservation query/reply packets. One widely-used random access protocol in RF networks is slotted Aloha (S-Aloha). Intuitively, since S-Aloha-RF is based on electromagnetic signal propagation, for short-range communication it is unaffected by propagation delay and delay variability. While S-Aloha-RF for terrestrial communication has been widely studied, S-Aloha for underwater networks is yet to be studied thoroughly.

1.1 Background literature

Underwater communication is acoustic signal based, which, unlike RF signal-based communications, is associated with high propagation delay and delay variability. There are several underwater MAC protocol variants available in the literature [3–17]. Among these some are variants of carrier sense multiple access (CSMA) [4, 11, 13]. In delay-aware probability based random access MAC protocol [15], every transmitter is assigned a transmission probability for the corresponding receiver. The mobility aware underwater MAC protocol in [16] focuses on the problem of the mobile node to collect data from underwater sensor networks. The hybrid MAC protocol in [14] is a multi-channel

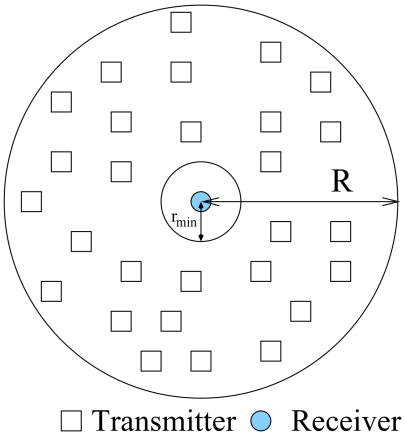

Fig. 1 *System model*

polling-based collision-free MAC protocol. In this protocol, the nodes are divided into groups. Corresponding to a group there is a channel reservation period to access the control channel. The number of data channels is as many as the number of groups in the system.

A set of works focused on S-Aloha-based protocols for underwater networks [3, 5–10, 17]. S-Aloha for underwater access can be divided in two categories: transmitter-synchronised [8] and receiver-synchronised [7, 9, 10]. In transmitter-synchronised S-Aloha, the transmitter sends data packets according to its own slot, i.e. the transmission is synchronised with respect to the transmitter's slot boundaries; it does not necessarily map to the slot boundaries at the receiver. On the other hand, in receiver-synchronised S-Aloha (RS-Aloha), the transmitter aims to send data packets in a way such that the packet reaches within a slot of the receiver. In the absence of propagation delay variability, RS-Aloha performance can be the same as that of S-Aloha-RF protocol. However, if there is a finite propagation delay between a transmitter and a receiver, without or with propagation delay variability, the performance of transmitter-synchronised S-Aloha with slot size equal to the packet transmission time can be as poor as Aloha protocol [6, 8, 9]. Considering an infinite number of nodes and modified slot size, the studies in [7, 9] showed that RS-Aloha generally performs better in environments with large propagation delay and propagation delay variability. In order to increase S-Aloha throughput with large propagation delay, frame-based S-Aloha with block acknowledgement (ACK) mechanism was proposed in [10]. These works do not address the stability issues in underwater environments with long and variable propagation delay.

The S-Aloha variant in [17] analytically captured the effect of retransmission. This protocol is frame based, where a frame consists of a time window for beaconing and a set of time slots for random access. At the start of every frame, the coordinator transmits the result of transmissions using the beacon, which contains information regarding the idle, collided, or successful slots in the previous frame. Thus, all the nodes receiving the beacon recognise the status of their transmission. The nodes having packets at the beaconing stage participate in the transmission process over the subsequent random access period. A node decides the instant of data packet transmission so that the packet can reach in a slot at the coordinator. The performance of this protocol is demonstrated using stability, throughput, and delay, which are parameterised in terms of transmission probability, retransmission probability, and frame size.

It is intuitive that the propagation delay variability would affect the performance of a MAC protocol [9, 18–20]. However, to the best of our knowledge, the performance of S-Aloha and other random access protocol variants for delay intensive environments, as discussed in the survey above, have not considered distance-dependent propagation delay variability and the associated stability issues in analysing the performance.

1.2 Motivation and key contributions

In view of the research gap stated above, it is our interest to parameterise stability performance of S-Aloha for underwater acoustic networks, accounting propagation delay variability, in addition to considering collision-related retransmission probability. Intuitively, to accommodate propagation delay variability, the slot size can be increased beyond the packet transmission time. For a given number of backlogged users, increased slot size can protect the inter-slot collision, but channel utilisation i.e. fraction of time slot used successfully for data packet transmission also decreases.

In this context, it needs to be studied how the interplay between inter-slot collision and channel utilisation would affect the stability performance of the RS-Aloha-based system, and an optimum slot size would be of interest to achieve a higher system performance.

Our key contributions in this study are as follows:

(a) Considering a finite number of unbuffered transmitters and transmitter–receiver distance-dependent propagation delay variability, we analyse the stability of RS-Aloha.
(b) From stability perspective we compare channel utilisation of RS-Aloha with respect to S-Aloha-RF.

1.3 Organisation

The rest of the paper is organised as follows. In Section 2, we describe the RS-Aloha with variable propagation delay to analyse stability issue. In Section 3, considering a finite number of unbuffered transmitters and transmitter–receiver distance-dependent delay variability, we analyse the stability of RS-Aloha. In Section 4, we compare channel utilisation of RS-Aloha and S-Aloha-RF from stability perspective. In Section 5, we conclude the paper.

2 RS-Aloha with variable propagation delay

The system model and assumptions are outlined here.

A many-to-one single-hop cluster scenario is considered, where the field nodes (transmitters) are uniformly randomly distributed around a sink (receiver) within its range $[r_{\min}, R]$. All the transmitters are located in a circular area around the receiver, which is positioned at the centre, as in Fig. 1. Thus, the area over which the transmitters are located is of size $\pi\left(R^2 - r_{\min}^2\right)$.

We consider that each transmitter can estimate its distance to the receiver [7, 9, 20], which is a reasonable assumption in underwater monitoring applications, such as sea-floor or river-bed deployments. Propagation delay is Gaussian distributed [9, 18–20]; we consider it has distance-dependent standard deviation $\sigma^{(r)}$. Motivated by the studies in [21–23], the nodes are considered full-duplex communication capable. Data packets are of fixed size with transmission time T_t. Reception error is due to MAC contentions and propagation delay-related synchronisation error. Fixed-sized feedback packet conveys a node's transmission status, which is considered error-free.

A simplified working mechanism of RS-Aloha protocol is depicted in Fig. 2. Time is divided in slots of size $T_s = T_t + \beta\sigma^{(R)}$, where β (≥ 0) is the controlling parameter for delay-collision trade-off. There are N stations, each of which can hold at most one packet at a time. Thus, before a successful transmission of a packet, a node does not generate any new packet. An unbacklogged node generates a packet in a slot with probability p. A successful packet is immediately acknowledged by the receiver. No ACK at the transmitter implies a collision. A collided packet is retransmitted by the backlogged transmitter with probability α in successive slots until its success. By the property of Gaussian distribution, a packet from a r distance away from the transmitter arrives at the receiver within $T_p^{(r)} \pm 3\sigma^{(r)}$ with 99.7% chance, where $T_p^{(r)}$ is the mean propagation delay from a transmitter at a distance r to the receiver.

Considering worst case propagation delay on either direction, the data packet length is chosen as $T_t \geq 2T_p^{(R)} + 6\sigma^{(R)}$, so that the data retransmission decision in the next slot can be taken by the

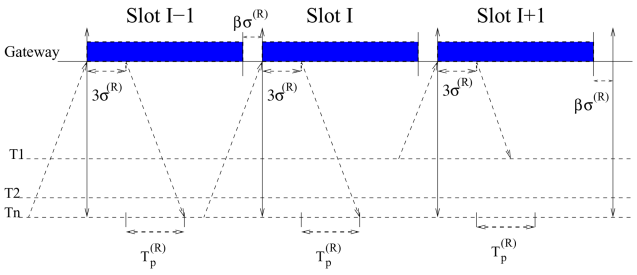

Fig. 2 *A simplified working mechanism of RS-Aloha*

end of the current slot. Note that the marginal chance of missed ACK due to delay variability beyond $+3\sigma^{(R)}$ is accounted by the optimum choice of β in deciding T_s.

A summary of notations used in this paper are listed in the Nomenclature section.

3 Channel utilisation and stability analysis

In this section, we analyse the performance of RS-Aloha considering a finite number of unbuffered transmitters. System state k is defined as the number of backlogged transmitters in it, which is monitored at the begining of a slot. There are total N transmitters. Success probability of a transmitted packet from a r-distance away node in system state k is given by (see (1))

A packet reaches the receiver at time y, which can vary in different slots. Considering the delay deviation factored in deciding T_s, y is restricted in $[(I-1)T_s, (I+1)T_s]$. r is in the range $[r_{\min}, R]$. A packet arriving in slot I can be new or a backlogged transmission, and it can be collided due to transmission in slot $I-1$ or $I+1$. $S_{I+1}()$ accounts for the effect of transmission in slot $I+1$. The second product term $[\cdot]$ in (1) accounts for the transmission in slot $I-1$. The state of slot $I-1$ can be $(k+1), k, \ldots, 0$, which is accounted in the success probability expression (1).

Before going into the detail description of (1), we use the notation $\boldsymbol{B}(n_b, m, \alpha, I)$ to indicate out of n_b backlogged transmitters m transmit, and $\boldsymbol{U}(n_u, m, p, I)$ to indicate out of n_u unbacklogged transmitters m transmit in slot I. $S_{I+1}(n_b)$ is the probability that none of the n_b backlogged transmitters in slot $I+1$ cause collision in slot I, given by

$$\begin{aligned} S_{I+1}(n_b) &= \left(\sum_{n=0}^{N-n_b} \boldsymbol{U}(N-n_b, n, p, I+1) \prod_{i_{p_n}=0}^{n} \{1-P_{I_n}\}\right) \\ &\quad \times \left(\sum_{m=0}^{n_b} \boldsymbol{B}(n_b, m, \alpha, I+1) \prod_{i_{p_m}=0}^{m} \{1-P_{I_n}\}\right) \\ &= \left(1-pP_{I_n}\right)^{N-n_b} \left(1-\alpha P_{I_n}\right)^{n_b}, \end{aligned} \tag{2}$$

where we have

$$\begin{aligned} \boldsymbol{B}(n_b, m, \alpha, I) &= \binom{n_b}{m} \alpha^m \left(1-\alpha\right)^{(n_b-m)}, \\ \boldsymbol{U}(n_u, m, p, I) &= \binom{n_u}{m} p^m \left(1-p\right)^{(n_u-m)}. \end{aligned} \tag{3}$$

Now we describe (1) in detail.

Case 1: State $k+1$ of slot $I-1$. For $(k+1)$ backlogged users in slot $I-1$, the state of slot I will be k, if 1 out of $(k+1)$ backlogged users transmit in slot $I-1$ and the transmission in slot $I-1$ does not reach at the receiver during $[y-T_t, y+T_t]$, where y is denoted as the time when the packet in slot I reaches the receiver. This probability expression can be written as

$$\begin{aligned} &\boldsymbol{U}(N-k-1, 0, p, I-1)\boldsymbol{B}(k+1, 1, \alpha, I-1) \\ &\times \left\{1-\Pr\left(y-T_t \le \boldsymbol{x}_{\boldsymbol{i_p}}(\boldsymbol{r}_{\boldsymbol{i_p}}) \le y+T_t\right)\right\} \\ &\quad = \boldsymbol{U}(N-k-1, 0, p, I-1)\boldsymbol{B}(k+1, 1, \alpha, I-1)\left\{1-P_{I_p}\right\}. \end{aligned} \tag{4}$$

Case 2: State k of slot $I-1$. For k backlogged users in slot $I-1$, the transmission in slot I is successfully received, when 2 or more out of k backlogged users transmit in slot $I-1$ and these packets do not reach at the receiver during $[y-T_t, y+T_t]$. Also, the transmission in slot I is successfully received, if there is zero or 1 transmission from the unbacklogged users in slot $I-1$ and this transmission in slot $I-1$ does not reach at the receiver during $[y-T_t, y+T_t]$. This probability expression is written as (see (5)) .

Case 3: State $k-1$ of slot $I-1$. For $k-1$ backlogged users in slot $I-1$, the transmission in slot I is received successfully, when 1 out of $N-k+1$ unbacklogged users transmit in slot $I-1$ and 1 or more out of $k-1$ backlogged users transmit in slot $I-1$, also the packet transmitted in slot $I-1$ does not reach at the receiver during $[y-T_t, y+T_t]$. This probability is expressed as

$$\begin{aligned} &\boldsymbol{U}(N-k+1, 1, p, I-1)\left\{1-P_{I_p}\right\}\left(\sum_{m=1}^{k-1} \boldsymbol{B}(k-1, m, \alpha, I-1)\right. \\ &\left.\times \prod_{i_{p_m}=0}^{m} \left\{1-P_{I_p}\right\}\right). \end{aligned} \tag{6}$$

Case 4: State $k-2$ to 0 of slot $I-1$. For $k-2$ backlogged users in slot $I-1$, the state in slot I is k, if the number of transmissions from unbacklogged users is 2 and zero or more number of transmission from backlogged users. Similarly, when the number of backlogged users is $k-3$ in slot $I-1$, the state of slot I will be k if the number of transmissions from unbacklogged users is 3, and so on. The transmission in slot I is received successfully if the transmission in slot $I-1$ does not reach the receiver during $[y-T_t, y+T_t]$. This probability expression is

$$\begin{aligned} P_s(k) = &\sum_{r=r_{\min}}^{R} \int_{y=(I-1)T_s}^{(I+1)T_s} \Big[\boldsymbol{U}(N-k, 1, p, I) S_{I+1}(k) \boldsymbol{B}(k, 0, \alpha, I) + \boldsymbol{U}(N-k, 0, p, I) S_{I+1}(k-1) \boldsymbol{B}(k, 1, \alpha, I)\Big] \\ &\times \Big[\boldsymbol{U}(N-k-1, 0, p, I-1)\boldsymbol{B}(k+1, 1, \alpha, I-1)\left\{1-P_{I_p}\right\} \\ &+\Big(\boldsymbol{U}(N-k, 0, p, I-1)\Big(\sum_{m=2}^{k} \boldsymbol{B}(k, m, \alpha, I-1) \prod_{i_{p_m}=0}^{m} \left\{1-P_{I_p}\right\}\Big) \\ &+\boldsymbol{B}(k, 0, \alpha, I-1) \cdot \Big(\boldsymbol{U}(N-k, 0, p, I-1) + \boldsymbol{U}(N-k, 1, p, I-1)\left\{1-P_{I_p}\right\}\Big)\Big) \\ &+\boldsymbol{U}(N-k+1, 1, p, I-1)\left\{1-P_{I_p}\right\} \sum_{m=1}^{k-1} \boldsymbol{B}(k-1, m, \alpha, I-1) \prod_{i_{p_m}=0}^{m} \left\{1-P_{I_p}\right\} \\ &+\sum_{m=0}^{k-2} \left(\Big(\boldsymbol{U}(N-m, k-m, p, I-1) \prod_{i_{p_m}=0}^{k-m} \left\{1-P_{I_p}\right\}\Big)\Big(\sum_{n=0}^{m} \boldsymbol{B}(m, n, \alpha, I-1) \prod_{i_{p_n}=0}^{n} \left\{1-P_{I_p}\right\}\Big)\right)\Big] \\ &\times \Pr(\boldsymbol{y_i} = y) \Pr(\boldsymbol{r_i} = r) \end{aligned} \tag{1}$$

$$\sum_{m=0}^{k-2}\Big(\Big(\boldsymbol{U}(N-m,k-m,p,I-1)\prod_{i_{p_m}=0}^{k-m}\big\{1-P_{I_p}\big\}\Big)\times\Big(\sum_{n=0}^{m}\boldsymbol{B}(m,n,\alpha,I-1)\prod_{i_{p_n}=0}^{n}\big\{1-P_{I_p}\big\}\Big)\Big). \tag{7}$$

Case 5: State k or $k-1$ of slot $I+1$. In slot $I+1$, the system state can be k or $k-1$. The transmission in slot I will be successfully received if the transmission in slot $I+1$ does not cause a collision. Also, the transmission in slot I is successfully received if there is only one transmission in slot I either from the backlogged users or from the unbacklogged users. This probability is expressed as

$$\begin{aligned}&\boldsymbol{U}(N-k,1,p,I)S_{I+1}(k)\boldsymbol{B}(k,0,\alpha,I)\\&\quad+\boldsymbol{U}(N-k,0,p,I)S_{I+1}(k-1)\boldsymbol{B}(k,1,\alpha,I).\end{aligned} \tag{8}$$

By considering all the above cases finally we can derive the probability of success, when the system state is k, as in (1).

Based on the field study data available in [18], we model the propagation delay as Gaussian distributed with distance-dependent propagation delay variation. In the context of RS-Aloha, a transmitter sends packet in a way that it is targeted to reach within a slot at the receiver. Here, propagation delay from any transmitter to the start of a slot at the receiver is Gaussian distributed with distance-dependent propagation delay variation. Consider, a transmitter sends a data packet at time t_i. Given that $\boldsymbol{T}_{\mathrm{p}}^{(r_i)}\sim\mathcal{N}\big(T_{\mathrm{p}},\sigma^{(r_i)^2}\big)$, we have $(t_i+\boldsymbol{T}_{\mathrm{p}}^{(r_i)})\sim\mathcal{N}\big(t_i+T_{\mathrm{p}},\sigma^{(r_i)^2}\big)$. Denote $t_i+T_{\mathrm{p}}=IT_{\mathrm{s}}$, i.e. a packet from a r_i distance away from the transmitter reaches the receiver (gateway) in slot I. Therefore, with the Gaussian-distributed $\boldsymbol{T}_{\mathrm{p}}^{(r_i)}$, packet arrival time at the receiver $\boldsymbol{x_i}(r_i)$, with IT_{s} as the start of Ith time slot, is given by

$$\boldsymbol{x_i}(r_i)\sim\mathcal{N}\big(IT_{\mathrm{s}},\sigma^{(r_i)^2}\big). \tag{9}$$

Similarly for the packet of the $(I-1)$th slot, $(I+1)$th slot and for the concerned packet of the Ith slot, respectively, we have

$$\begin{aligned}\boldsymbol{x_{i_p}}(r_{i_p})&\sim\mathcal{N}\big((I-1)T_{\mathrm{s}},\sigma^{(r_{i_p})^2}\big);\\\boldsymbol{x_{i_n}}(r_{i_n})&\sim\mathcal{N}\big((I+1)T_{\mathrm{s}},\sigma^{(r_{i_n})^2}\big);\\\boldsymbol{y_i}(r_i)&\sim\mathcal{N}\big(IT_{\mathrm{s}},\sigma^{(r_i)^2}\big).\end{aligned} \tag{10}$$

We consider $R=r_{\min}+\delta\times n_s$, where δ is the difference between two consecutive values of transmitter–receiver distance. We define transmitter–receiver distance as discrete uniform distribution, which takes value from $\{r_{\min},r_{\min}+\delta,\ldots,R\}$. Thus $\Pr(\boldsymbol{r_i}=r)$ is defined as [24]

$$\Pr(r_i=r)=\frac{1}{n_s+1}. \tag{11}$$

From Section 2 we recall that propagation delay deviation $\sigma^{(r)}$ is a function of transmitter–receiver distance r has not been characterised so far in the literature. To incorporate this distance factor, in this study, we consider that the standard deviation $\sigma^{(r)}$ of delay is of a generic form $\sigma^{(r)}=c(r/v)^q$, where r is the transmitter-to-receiver distance, $c,q\geq 0$ are constants representing the nature of delay variability, and v is the underwater acoustic signal propagation speed. q is called delay variability exponent. For $\frac{r}{v}<1$, $\sigma^{(r)}$ decreases with the increase of q. Also, with the increase of c, $\sigma^{(r)}$ increases.

With this consideration, P_{I_p}, P_{I_n} are obtained as

$$\begin{aligned}P_{I_p}&=\Pr\big(y-T_{\mathrm{t}}\leq\boldsymbol{x_{i_p}}(\boldsymbol{r_{i_p}})\leq y+T_{\mathrm{t}}\big)\\&=\sum_{r=r_{\min}}^{R}\Pr(y-T_{\mathrm{t}}\leq\boldsymbol{x_{i_p}}(\boldsymbol{r_{i_p}}=r)\leq y+T_{\mathrm{t}})\cdot\Pr(\boldsymbol{r_{i_p}}=r)\\&=\sum_{r=r_{\min}}^{R}\frac{1}{2}\Big[\mathrm{erf}\Big(\frac{y+T_{\mathrm{t}}-(I-1)T_{\mathrm{s}}}{\sigma^{(r)}\sqrt{2}}\Big)\\&\quad-\mathrm{erf}\Big(\frac{y-T_{\mathrm{t}}-(I-1)T_{\mathrm{s}}}{\sigma^{(r)}\sqrt{2}}\Big)\Big]\frac{1}{n_s+1}.\end{aligned} \tag{12}$$

$$\begin{aligned}P_{I_n}&=\Pr\big(y-T_{\mathrm{t}}\leq\boldsymbol{x_{i_n}}(\boldsymbol{r_{i_n}})\leq y+T_{\mathrm{t}}\big)\\&=\sum_{r=r_{\min}}^{R}\Pr(y-T_{\mathrm{t}}\leq\boldsymbol{x_{i_n}}(\boldsymbol{r_{i_n}}=r)\leq y+T_{\mathrm{t}})\cdot\Pr(\boldsymbol{r_{i_n}}=r)\\&=\sum_{r=r_{\min}}^{R}\frac{1}{2}\Big[\mathrm{erf}\Big(\frac{y+T_{\mathrm{t}}-(I+1)T_{\mathrm{s}}}{\sigma^{(r)}\sqrt{2}}\Big)\\&\quad-\mathrm{erf}\Big(\frac{y-T_{\mathrm{t}}-(I+1)T_{\mathrm{s}}}{\sigma^{(r)}\sqrt{2}}\Big)\Big]\frac{1}{n_s+1}.\end{aligned} \tag{13}$$

For the derivation of the above, we have used the identities:

$$\mathrm{erf}(x)=\frac{2}{\sqrt{\pi}}\int_0^x\mathrm{e}^{-t^2}\mathrm{d}t,\quad\text{and}\quad\int_a^b\frac{1}{\sigma\sqrt{2\pi}}\mathrm{e}^{-\frac{1}{2}\left(\frac{x-\mu}{\sigma}\right)^2}\mathrm{d}x=\frac{1}{2}\Big[\mathrm{erf}\Big(\frac{b-\mu}{\sigma\sqrt{2}}\Big)-\mathrm{erf}\Big(\frac{a-\mu}{\sigma\sqrt{2}}\Big)\Big]. \tag{14}$$

Substituting the above and simplifying, (1) reduces to (see (15))

Channel utilisation, i.e. the fraction of the slot used for sending data successfully, is defined as

$$\eta=\frac{T_{\mathrm{t}}}{T_{\mathrm{s}}}\times P_{\mathrm{s}}(k)=\frac{T_{\mathrm{t}}P_{\mathrm{s}}(k)}{T_{\mathrm{t}}+\beta\sigma^{(R)}}. \tag{16}$$

It should be noted that, in (16), $\beta=0$ does not imply channel utilisation η is maximum, because with $\beta=0$, $P_{\mathrm{s}}(k)$ is very low, and most of the packets encounter collision. Therefore, a maximum value of $P_{\mathrm{s}}(k)$ is obtained by choosing an optimum value of β. Without an optimum value of β, it might be possible that $P_{\mathrm{s}}(k)$ is maximum but the utilisation is low due to the high value of β.

3.1 Maximisation of utilisation

We note that a right choice of β (hence slot size) is needed so that the utilisation η is maximised. We formulate an optimisation problem to maximise η for the given values of T_{t}, $\sigma^{(R)}$, p, and α.

$$\underset{\beta}{\text{Maximise:}}\ \eta=\frac{T_{\mathrm{t}}P_{\mathrm{s}}(k)}{T_{\mathrm{t}}+\beta\sigma^{(R)}}. \tag{17}$$

With an optimum value of β inter-slot collision of the packet is eliminated. Then, the state transition probability similarly obtained as in [25]. From transition probabilities, system state probabilities can be obtained. This discussion is however out of the scope of this work.

The drift in state k is defined in (18), where $(N-k)p$ is the traffic generated from the unbacklogged nodes, which can also be considered as the system load. $(N-k)p$ is called the load line,

$$\boldsymbol{U}(N-k,0,p,I-1)\Big(\sum_{m=2}^{k}\boldsymbol{B}(k,m,\alpha,I-1)\prod_{i_{p_m}=0}^{m}\big\{1-P_{I_p}\big\}\Big)+\boldsymbol{B}(k,0,\alpha,I-1)\Big(\boldsymbol{U}(N-k,0,p,I-1)+\boldsymbol{U}(N-k,1,p,I-1)\big\{1-P_{I_p}\big\}\Big). \tag{5}$$

$$
\begin{aligned}
P_s(k) = \sum_{r=r_{\min}}^{R} \int_{y=(I-1)T_s}^{(I+1)T_s} & \Big[(N-k)p(1-p)^{N-k-1}(1-\alpha)^k S_{I+1}(k) + (1-p)^{N-k}k\alpha(1-\alpha)^{k-1}S_{I+1}(k-1)\Big] \\
& \times \Big[(1-p)^{N-k-1}(k+1)\alpha(1-\alpha)^k\big(1-P_{I_p}\big) + (1-p)^{N-k} \\
& \times \sum_{m=2}^{k}\binom{k}{m}\alpha^m(1-\alpha)^{k-m}\big(1-P_{I_p}\big)^m + (N-k+1)p(1-p)^{N-k}\big(1-P_{I_p}\big) \\
& \times \sum_{m=1}^{k-1}\binom{k-1}{m}\alpha^m(1-\alpha)^{k-m-1}\big(1-P_{I_p}\big)^m \\
& + \sum_{m=0}^{k-2}\Big(\binom{N-m}{k-m}p^{k-m}(1-p)^{N-k}\big(1-P_{I_p}\big)^{k-m}\big(1-\alpha P_{I_p}\big)^m\Big)\Big]\frac{e^{-\frac{1}{2}\left(\frac{y-IT_s}{c\left(\frac{r}{v}\right)^q}\right)^2}}{\sqrt{2\pi}c\left(\frac{r}{v}\right)^q}\cdot\frac{1}{n_s+1}\mathrm{d}y
\end{aligned}
\tag{15}
$$

Table 1 Default underwater communication system parameters

packet size	1200 bytes
mean signal propagation speed (v)	1500 m/s
communication bandwidth (b_w)	16 kbps
maximum nodal communication range (R)	100 m
minimum nodal communication range ($r_{\min}$)	1 m
total users in the system (N)	150
propagation delay variability exponent (q)	1

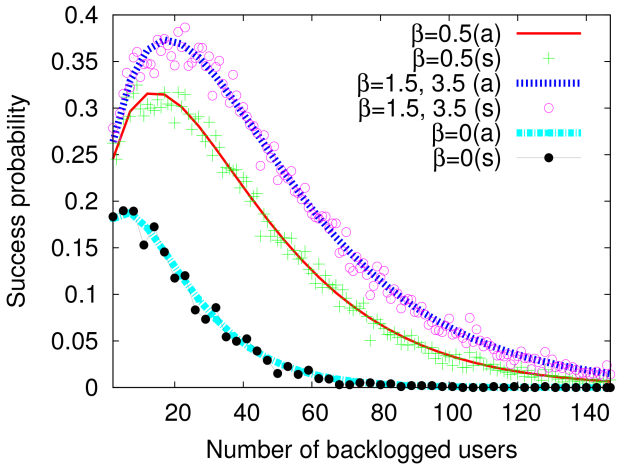

Fig. 3 *Probability of success comparison for various values of slot increment factor of RS-Aloha. Data packet size 1200 bytes, $p = 0.002$, $\alpha = 0.04$, $R = 100\,m$, $c = 0.7$, $q = 1$*

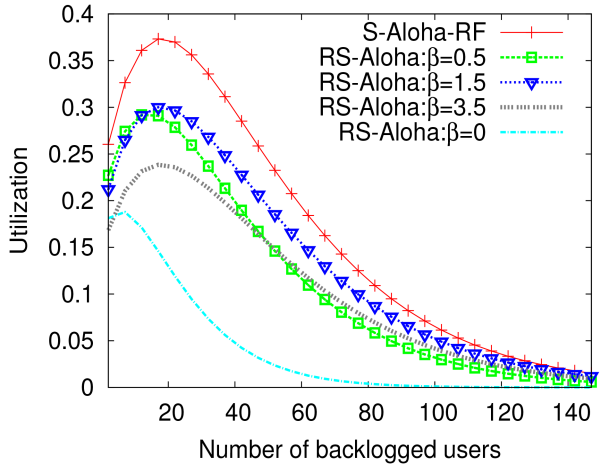

Fig. 4 *Performance comparison for various values of slot increment factor. Data packet size 1200 bytes, $p = 0.002$, $\alpha = 0.04$, $R = 100\,m$, $c = 0.7$, $q = 1$*

where N is the total number of users in the system, k is the number of backlogged users, p is the transmission probability of an unbacklogged user. For $k = 0$, the load line has maximum value Np. For $k = N$, the load line has minimum value, i.e. 0

$$
D_k = (N-k)p - \frac{T_t P_s(k)}{T_t + \beta^{opt}\sigma^{(R)}}. \tag{18}
$$

For $D_k = 0$, the system is in equilibrium. The system is unstable if $D_k > 0$ because transmissions from unbacklogged nodes are not successful, and hence the number of backlogged packets continue to grow. On the other hand, for $D_k < 0$ the system is stable.

4 Results and discussion

To generate results, we consider the value of common parameters as in Table 1. Data packet size is selected such that $T_t \geq 2T_p^{(R)} + 6\sigma^{(R)}$. With this consideration, in this work, we have used 1200 bytes as packet size while carrying out simulation-based performance studies. The consideration of 1200 bytes packet size is also motivated by the prior underwater acoustic networks studies in [26, 27]. With the assumption of no buffering at the transmitters, to account for the prompt delivery of backlogged packets, the new arrival probability p is considered small relative to backlog transmission probability α, i.e. $p \ll \alpha$. Accordingly, in a slot, an unbacklogged transmitter generates a packet with probability $p = 0.002$ and backlogged transmitter retransmits a failed packet with probability $\alpha = 0.04$. The numerical results are generated using Scilab [28]. All results (except Figs. 3 and 4) are with an optimum value of slot increment factor β that offers the maximum channel utilisation given by (17), and the results are verified by discrete event simulations in C language. To generate simulation result, we have written simulation programme using C language and executed in Linux, where for a given value of minimum distance ($r_{\min}$) and maximum distance (R) between receiver and transmitters, we generate uniform random distance between receiver and transmitters. Then this generated distance is rounded off to the nearest integer. Now depending on the generation probability, nodes transmit in such a way that the packet can be received in a slot at the receiver. Simulations were repeated for 1000 consecutive slots and the process was iterated 2000 times. For the numerical results, we use the difference between two consecutive values of transmitter–receiver distance (δ) as 1. In all the figures with the required verification of analysis and simulations, we have denoted the analytical results by '(a)', whereas the simulation results denoted by '(s)'. The plots having only analytical results (to avoid the clutter of multiple repeated simulation-based verifications) do not contain this additional notation. In addition to showing the performance results of RS-Aloha in underwater acoustic networks, we show the corresponding S-Aloha-RF performance result as well, as expressed in (19), which is unaffected by propagation delay and propagation delay variability for communication over the same short-range communication. The S-Aloha-RF performance results clearly contrast the effect of underwater signal propagation speed on the system utilisation and stability aspects.

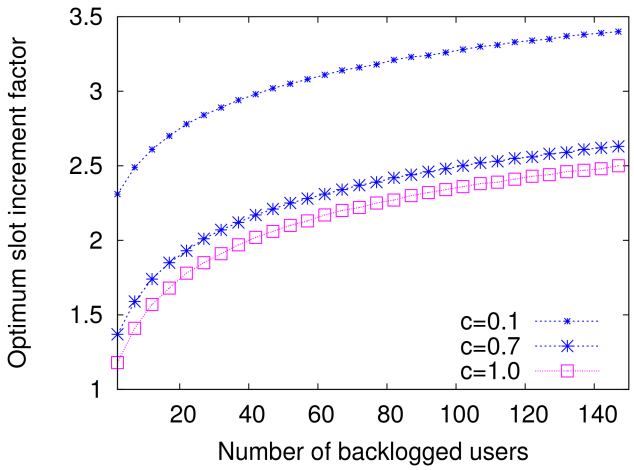

Fig. 5 *Optimum slot increment factor β^{opt} versus traffic load. Packet size 1200 bytes, communication range $R = 100\,m$, new generation probability $p = 0.002$, backlog retransmission probability $\alpha = 0.04$, and delay variability exponent $q = 1$*

Following [25, Ch. 4], utilisation in S-Aloha-RF is given by

$$\eta^{\mathrm{RF}} = (N-k)p(1-p)^{(N-k-1)}(1-\alpha)^{k} + k\alpha(1-\alpha)^{(k-1)}(1-p)^{(N-k)}. \tag{19}$$

Correspondingly, drift in S-Aloha-RF is given by

$$D_k^{\mathrm{RF}} = (N-k)p - \eta^{\mathrm{RF}}. \tag{20}$$

First, in Fig. 3, we show the probability of success to receive a packet for various values of β. Here, it can be observed that for a low value of β due to the inter-slot collision, the probability of success is low. However, for a high value of β, we note that the probability of success has reached as maximum as possible. Now for the same value of β, the utilisation performance is presented in Fig. 4. The importance of finding the optimum slot increment factor can be noted from Figs. 3 and 4. Owing to the increase of slot increment factor β, the utilisation increases until a certain value of β and then decreases due to less use of time resource for data transmission purpose, i.e. if the value of β is increased, the probability of success increases, but a fraction of time per slot used to transmit data is less. Thus, the utilisation decreases at a large value of β. Therefore, the optimum value of slot increment factor β^{opt} is needed for maximum utilisation. From Fig. 4 it can be observed that with $\beta = 0$ (i.e. slot size $T_s = T_t$) utilisation of RS-Aloha is the same as that of the pure Aloha protocol, which again corroborates the observation in Fig. 3 that inter-slot collision due to propagation delay and delay variability degrades the performance of RS-Aloha to that of pure Aloha. From Fig. 4 the difference between the S-Aloha-RF and RS-Aloha is apparent from the utilisation perspective. In the subsequent discussions, we consider β^{opt} that offers maximum utilisation of RS-Aloha.

4.1 Effect of delay variability

To study channel utilisation with respect to delay variability constant c, we consider packet size 1200 bytes, communication range $R = 100$ m, and $q = 1$. First, Fig. 5 shows the optimum slot increment factor β^{opt} for achieving the maximum utilisation at various backlog conditions. With more backlogged users, i.e. at a higher value of k, collision probability and the effect of delay variability is more prominent. For a given c, a higher value of β helps mitigate these collisions, which explains the monotonically increasing β^{opt} with k. At a higher value of c, a small value of β is required to maximise the utilisation, which is the product of fraction of slot used for data transmission and success probability. A large value of c contributes to the increase of T_s. Therefore, to get the maximum utilisation, the value of β needs to be kept low.

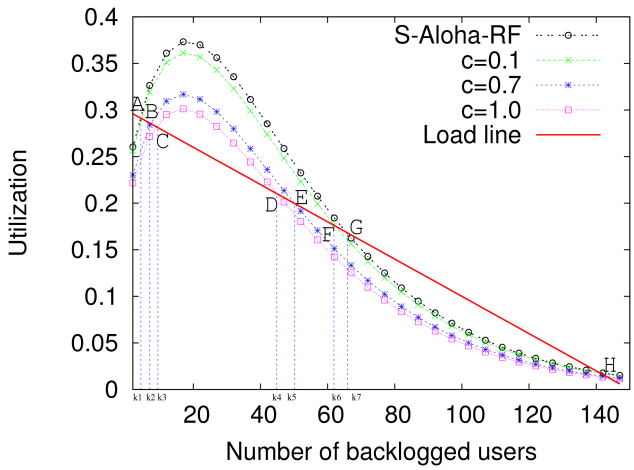

Fig. 6 *Maximum channel utilisation at various values of delay variability constant. Data packet size 1200 bytes, $R = 100\,m$, $p = 0.002$, $\alpha = 0.04$, and $q = 1$. Stable points are A, B, C. Unstable points are D, E, F, G*

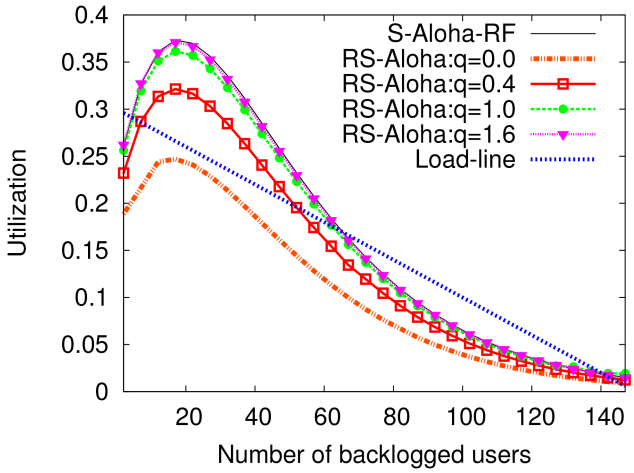

Fig. 7 *Performance comparison with respect to delay variability exponent. Data packet size 1200 bytes, $R = 100\,m$, $p = 0.002$, $\alpha = 0.04$, $c = 0.1$*

For a given value of c, with the increase of k, the optimum slot increment factor increases to get the maximum utilisation.

Fig. 6 shows utilisation versus system load at different values of c. For any value of c the utilisation is maximum at system state $k = 20$, because at $k = 20$ the number of arrivals per slot $(N-k)p + k\alpha \simeq 1$. Note that, while S-Aloha-RF is unaffected by propagation delay variability, in RS-Aloha a higher delay variability (higher value of c) causes a lower utilisation. For a higher value of c, the system's stable operation region shrinks. For example, at $c = 0.1$ the unstable equilibrium point is at k_6, whereas at $c = 1.0$ it shrinks to k_4.

4.2 Effect of delay variability exponent

To compare utilisation with respect to delay variability exponent q, in Fig. 7, we consider packet size 1200 bytes, transmission range $R = 100$ m, transmission probability $p = 0.002$, retransmission probability $\alpha = 0.04$ and propagation delay variability constant $c = 0.1$. For a large value of the exponent, $q = 1.6$, delay deviation is much smaller. Therefore the utilisation is high and close to the utilisation of S-Aloha-RF. However, for the low value of the exponent, $q = 0.4$, the delay deviation is high, which causes the utilisation to be significantly less than S-Aloha-RF (which is unaffected by q). Here with the changes in the value of q, stable point and unstable point change in RS-Aloha. For low value, $q = 0.4$, the system's stable operation region shrinks significantly. With $q = 0$ and $c = 0.1$, $\sigma^{(r)} = 0.1$, there is no stability point in RS-Aloha.

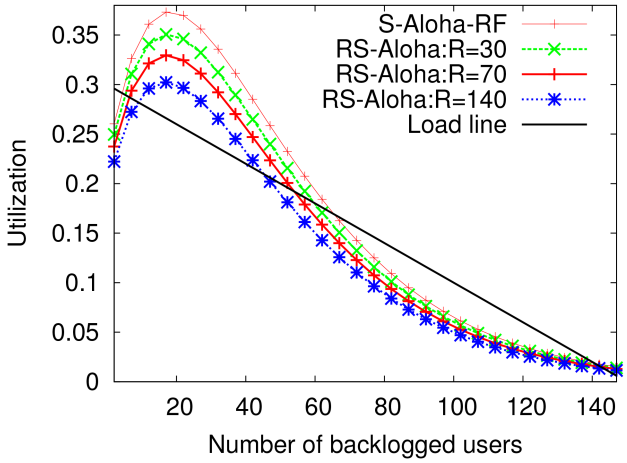

Fig. 8 *Utilisation for various values of communication range. Data packet size 1200 bytes, $p = 0.002$, $\alpha = 0.04$, $c = 0.7$, and $q = 1$*

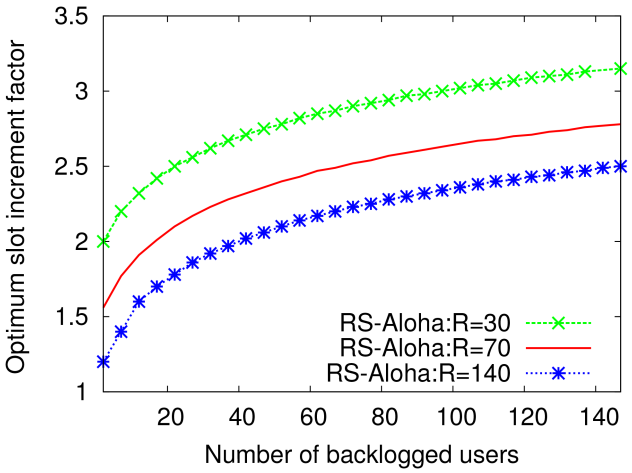

Fig. 9 *Optimum slot increment factors corresponding to backlogged users for a given value of transmission range. Data packet size 1200 bytes, $p = 0.002$, $\alpha = 0.04$, $c = 0.7$, and $q = 1$*

4.3 Effect of communication range

To study utilisation as a function of communication range R, we consider packet size 1200 bytes (to ensure $T_t \geq 2T_p^{(R)} + 6\sigma^{(R)}$ for all chosen values of R), $p = 0.002$, $\alpha = 0.04$, $c = 0.7$, and $q = 1$. The plots in Fig. 8 show that the utilisation decreases with the increase of R. For a high value of R, the delay deviation is high. Therefore, a useful time for data transmission per slot reduces. Owing to the decreased utilisation at high value of R, the stability region also shrinks, as the stable equilibrium point and unstable equilibrium point approach each other. From this figure, it can also be observed that the S-Aloha-RF is unaffected by the communication range R.

The optimum slot increment factors corresponding to Fig. 8 is also plotted in Fig. 9. In this figure, we observe that with the increase of backlogged users the optimum value of slot increment factor increases for a given value of transmission range. Also, for a longer transmission range, a smaller value of slot increment factor is required. The trend here is similar to that of Fig. 5.

4.4 Effect of network traffic intensity

To study utilisation as a function of retransmission probability α, we consider packet size as 1200 bytes, propagation delay variability constant $c = 0.7$ and exponent $q = 1$, transmission probability $p = 0.002$, communication range $R = 100$ m. In Fig. 10, we evaluate utilisation and stability for retransmission probability $\alpha = 0.013, 0.04, 0.171$. For $\alpha = 0.171$, with the increase of backlogged users k, the number of arrivals per slot increases, as a result the utilisation is decreasing. Stability of the system for various values of retransmission probability α is also clearly visible

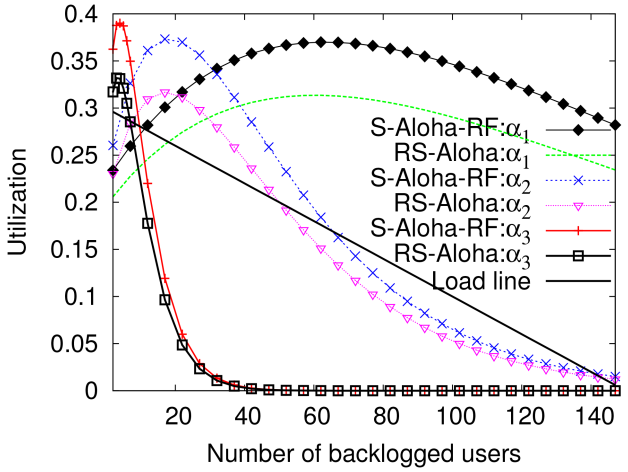

Fig. 10 *Utilisation performance at various values of retransmission probability $\alpha_1 = 0.013, \alpha_2 = 0.04, \alpha_3 = 0.171$. Data packet size 1200 bytes, $p = 0.002$, $R = 100$ m, $c = 0.7$, and $q = 1$*

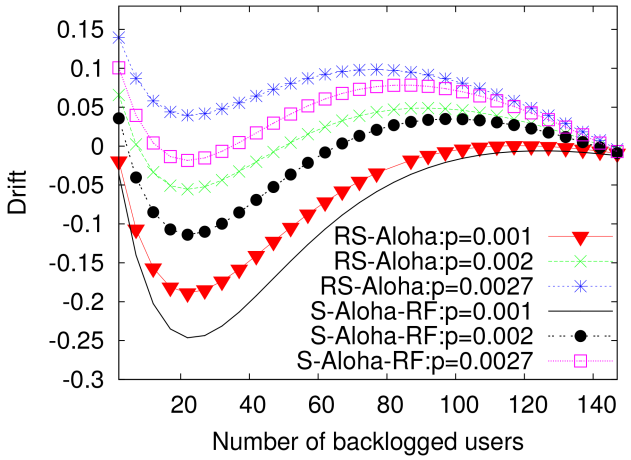

Fig. 11 *Stability performance comparison for various values of transmission probability. Data packet size 1200 Bytes, $\alpha = 0.04$, $R = 100$ m, $c = 0.7$, $q = 1$*

from the intersection of the load line with the utilisation plot. This figure also demonstrates that the performance of S-Aloha-RF is always higher than that of RS-Aloha, which is because of negligible propagation delay variability of RF signals. The change of stability regions of RS-Aloha and S-Aloha-RF can be clearly noted from this figure. For $\alpha = 0.04$, the S-Aloha-RF is stable till $k = 67$, but RS-Aloha is stable till $k = 57$. The change of stability points is visible for other values of α as well. The stability points of RS-Aloha differ from S-Aloha-RF because the utilisation of RS-Aloha decreases due to the increase of collision in the presence of propagation delay deviation.

4.5 Stability performance

Finally, Fig. 11 exclusively captures the stability performance of RS-Aloha relative to S-Aloha-RF in terms of drift at different new arrival probability. To compare drift with respect to transmission probability p we consider data packet size 1200 bytes, $c = 0.7$, $q = 1$, retransmission probability $\alpha = 0.04$, communication range $R = 100$ m. The transmission probabilities considered are $p = 0.001, 0.002, 0.0027$. With $p = 0.001$, we have a stability region (where drift is negative) for RS-Aloha, but there is no stability region with a higher transmission probability of $p = 0.0027$. S-Aloha-RF, on the other hand, has a stability region even at that high transmission probability $p = 0.0027$. For $p = 0.002$, RS-Aloha system is stable till the number of backlogged users is 50. For the same value of p, S-Aloha-RF system is stable till the number of backlogged users are 70. The difference in stability points of RS-Aloha is due to the presence of

distance-dependent propagation delay deviation. In the presence of propagation delay deviation, the collision increases, and utilisation decreases. So the stability point changes for RS-Aloha in underwater acoustic networks.

5 Concluding remarks

We have presented stability analysis of RS-Aloha in underwater acoustic networks, where propagation delay and delay variability are not negligible. In the analysis, we have considered a finite number of unbuffered transmitters with retry for the failed transmissions. We have compared the utilisation of RS-Aloha and S-Aloha-RF from a stability perspective. We have shown through mathematical analysis, supported by discrete event simulations, that channel utilisation, as well as stability region in RS-Aloha, are significantly influenced by communication range, delay variability factors, new transmission probabilities, and backlogged retransmission probabilities. The study can be useful in designing cluster-based underwater acoustic networks.

6 References

[1] Urick, R.J.: '*Principles of underwater sound*' (McGraw-Hill, New York, USA, 1983)

[2] Casari, P., Zorzi, M.: 'Protocol design issues in underwater acoustic networks', *Comput. Commun.*, 2011, **34**, (17), pp. 2013–2025

[3] Vieira, L.F.M., Kong, J., Lee, U., *et al.*: 'Analysis of Aloha protocols for underwater acoustic sensor networks'. Proc. ACM Workshop on UnderWater Networks (WUWNET), Los Angeles, CA, USA, 2006, pp. 1–2

[4] Ng, H.H., Soh, W.S., Motani, M.: 'ROPA: a MAC protocol for underwater acoustic networks with reverse opportunistic packet appending'. Proc. IEEE Wireless Communications and Networking Conf. (WCNC), Sydney, Australia, 2010, pp. 1–6

[5] Xiao, Y., Zhang, Y., Gibson, J.H., *et al.*: 'Performance analysis of ALOHA and p-persistent ALOHA for multi-hop underwater acoustic sensor networks', *Cluster Comput.*, 2011, **14**, (1), pp. 65–80

[6] De, S., Mandal, P., Chakraborty, S.S.: 'On the characterization of Aloha in underwater wireless networks', *Math. Comput. Modell.*, 2011, **53**, (11-12), pp. 2093–2107

[7] Zhou, Y., Chen, K., He, J., *et al.*: 'Enhanced slotted Aloha protocols for underwater sensor networks with large propagation delay'. Proc. IEEE VTC Spring, Budapest, Hungary, 2011, pp. 1–5

[8] Ahn, J., Syed, A., Krishnamachari, B., *et al.*: 'Design and analysis of a propagation delay tolerant ALOHA protocol for underwater networks', *Ad Hoc Netw.*, 2011, **9**, (5), pp. 752–766

[9] Mandal, P., De, S., Chakraborty, S.S.: 'A receiver synchronized slotted Aloha for underwater wireless networks with imprecise propagation delay information', *Ad Hoc Netw.*, 2013, **11**, (4), pp. 1443–1455

[10] Baek, H., Lim, J., Oh, S.: 'Beacon-based slotted Aloha for wireless networks with large propagation delay', *IEEE Commun. Lett.*, 2013, **17**, (11), pp. 2196–2199

[11] Zhang, J., Qiao, G., Wang, C.: 'A distance aware protocol for underwater acoustic communication networks'. Proc. National Doctoral Academic Forum on Information and Communications Technology, Beijing, China, 2013, pp. 1–6

[12] Zhao, Q., Lambert, A., Benson, C.R.: 'FS-MACA: a future scheduling mac protocol in underwater acoustic networks'. Proc. ACM Workshop on UnderWater Networks (WUWNet), Rome, Italy, 2014, pp. 1–5

[13] Lee, J.W., Cho, H.S.: 'A hybrid sender- and receiver-initiated protocol scheme in underwater acoustic sensor networks', *Sensors*, 2015, **15**, (11), pp. 28052–28069

[14] Yang, M., Gao, M., Foh, C.H., *et al.*: 'Hybrid collision-free medium access protocol for underwater acoustic networks: design and performance evaluation', *IEEE J. Ocean. Eng.*, 2015, **40**, (2), pp. 292–302

[15] Han, Y., Fei, Y.: 'A delay-aware probability-based mac protocol for underwater acoustic sensor networks'. Proc. Int. Conf. on Computing, Networking, and Communications, Garden Grove, CA, USA, 2015, pp. 938–944

[16] Gao, B., Zhang, L., Chu, D., *et al.*: 'A novel mobility aware medium access control protocol for underwater sensor networks'. Proc. IEEE OCEANS, Shanghai, China, 2016, pp. 1–6

[17] Baek, H., Lim, J.: 'Performance analysis of block ACK-based slotted ALOHA for wireless networks with long propagation delay', *Ad Hoc Netw.*, 2016, **42**, pp. 34–46

[18] Stojanovic, M.: '*Acoustic underwater communications. Encyclopedia of telecommunications*' (John Wiley and Sons, New York, USA, 2003)

[19] Pompili, D., Melodia, T., Akyildiz, I.F.: 'Routing algorithms for delay-insensitive and delay-sensitive applications in underwater sensor networks'. ACM MobiCom, Los Angeles, CA, USA, 2006, pp. 298–309

[20] Mandal, P., De, S.: 'New reservation multiaccess protocols for underwater wireless ad hoc sensor networks', *IEEE J. Oceanic Eng.*, 2015, **40**, (2), pp. 277–291

[21] Gibson, J., Larraza, A., Rice, J., *et al.*: 'On the impacts and benefits of implementing full-duplex communication links in an underwater acoustic network'. Proc. Int. Mine Symp., Monterey, CA, USA, 2002, pp. 1–10

[22] Peleato, B., Stojanovic, M.: 'A channel sharing scheme for underwater cellular networks'. Proc. IEEE OCEANS, Aberdeen, Europe, 2007, pp. 1–5

[23] Zhang, J., Ma, X., Qiao, G., *et al.*: 'A full-duplex based protocol for underwater acoustic communication networks'. Proc. IEEE OCEANS, San Diego, CA, USA, 2013, pp. 1–6

[24] Papoulis, A., Pillai, S.U.: '*Probability, random variables, and stochastic processes*' (Tata McGraw-Hill Editions, New Delhi, 2002, 4th edn.)

[25] Bertsekas, D., Gallager, R.: '*Data networks*' (Prentice-Hall, New Jersey, USA, 1992, 2nd edn.)

[26] Yildiz, H.U., Gungor, V.C., Tavli, B.: 'Packet size optimization for lifetime maximization in underwater acoustic sensor networks', *IEEE Trans. Ind. Inf.*, 2019, **15**, (2), pp. 719–729

[27] Basagni, S., Petrioli, C., Petroccia, R., *et al.*: 'Optimized packet size selection in underwater wireless sensor network communications', *IEEE J. Ocean. Eng.*, 2012, **37**, (3), pp. 321–337

[28] Enterprises, S.: '*Scilab: free and open source software for numerical computation*' (Scilab Enterprises, Orsay, France, 2017). Available at http://www.scilab.org